

## Electronic Supplementary Information

### A General Synthetic Approach for Hexagonal Phase Tungsten Nitride Composites and Their Application in the Hydrogen Evolution Reaction

Haiyan Jin<sup>†</sup>, Hao Zhang<sup>‡</sup>, Jiayi Chen<sup>†</sup>, Shanjun Mao<sup>†</sup>, Zheng Jiang<sup>‡\*</sup> and Yong Wang<sup>†\*</sup>

<sup>†</sup>Advanced Materials and Catalysis Group, Institute of Catalysis, Zhejiang University, Hangzhou 310028, P. R. China.

<sup>‡</sup>Shanghai Institute of Applied Physics, Chinese Academy of Sciences, Shanghai 201204, P. R. China.

#### EXPERIMENTAL SECTION

**Materials.** cobalt(II) nitrate hexahydrate ( $\text{Co}(\text{NO}_3)_2 \cdot 6\text{H}_2\text{O}$ ), 2-methylimidazole, ammonium metatungstate (AMT), 20% Pt/C, anhydrous methanol, potassium hydroxide (KOH), 5 wt.% Nafion 117 solution were purchased from Aladdin. They were all used as received without further purification.

**Preparation of W-based composites.** In a typical synthesis process, 6 mmol AMT was dissolved in 60 mL methanol. 3.94 g 2-methylimidazole was also dissolved in 40 mL methanol and then added slowly into the former solution with strong stirring. After the mixture was incubated at room temperature for 24 h, the as-obtained precipitate was centrifuged and washed with ethanol for several times. After that the mixture was heated overnight at 70 °C in drying oven to remove the water and then the dry mixture was grinded finely. The as-prepared W precursors were further heated in a tube furnace at 600-800 °C for 60 min under flowing 400 sccm ammonia gas with a heating rate of 5 °C min<sup>-1</sup> and cooled down naturally to room temperature and then  $\beta$ -WN at different calcination procedure could be acquired. The variation of  $\beta$ -WN phase is presented in Figure S1. The change of 2-methylimidazole during nitridation process is difficult to be studied, because 2-methylimidazole without cobalt and AMT is unstable and volatile at high temperature.

**Preparation of  $\beta$ -WN/Co<sub>2.45</sub>.** Mixing the materials metal Co prepared under the procedure of WN/Co synthesis and  $\beta$ -WN at the ratio of 2.45:1 and grinding. The preparation of  $\beta$ -WN/Ni and  $\beta$ -WN/Fe is similar to  $\beta$ -WN/Co<sub>2.45</sub> except that the ratio of Ni or Fe and  $\beta$ -WN is 5.

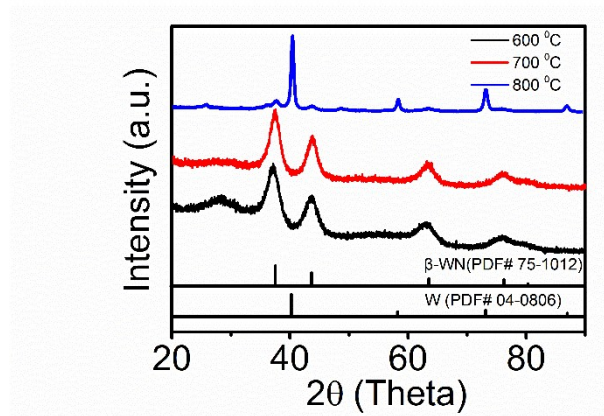


**Figure S1.** X-ray diffraction patterns of  $\beta$ -WN at different calcined temperature.

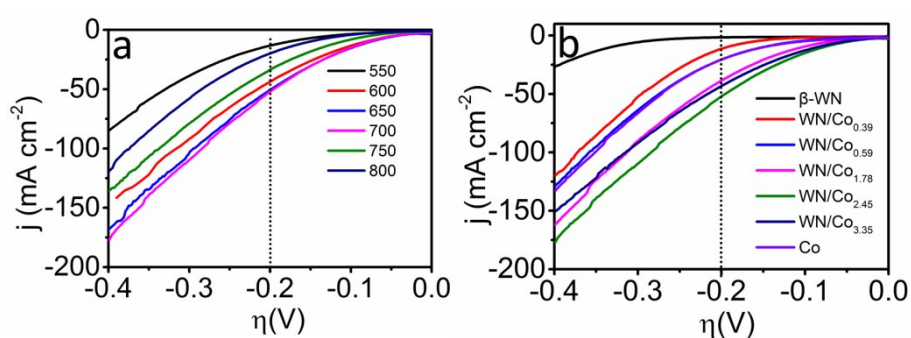


**Figure S2.** Polarization curves of WN/Co hybrids a) at different calcination temperature and b) at different Co/W ratio.

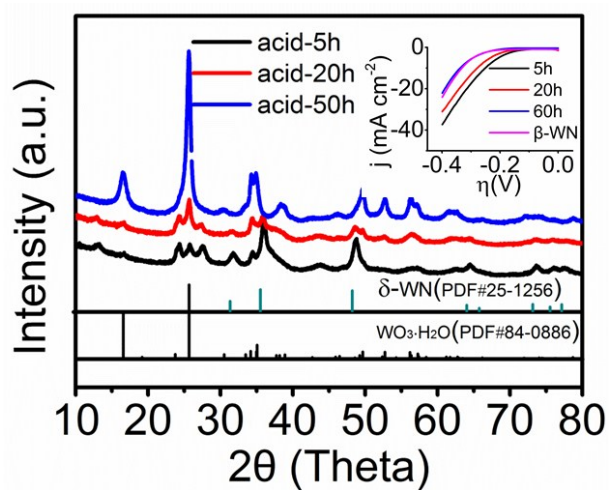


**Figure S3.** X-ray diffraction patterns and polarization curves in inset of  $\delta$ -WN/Co<sub>2.45</sub> after acid treatment.

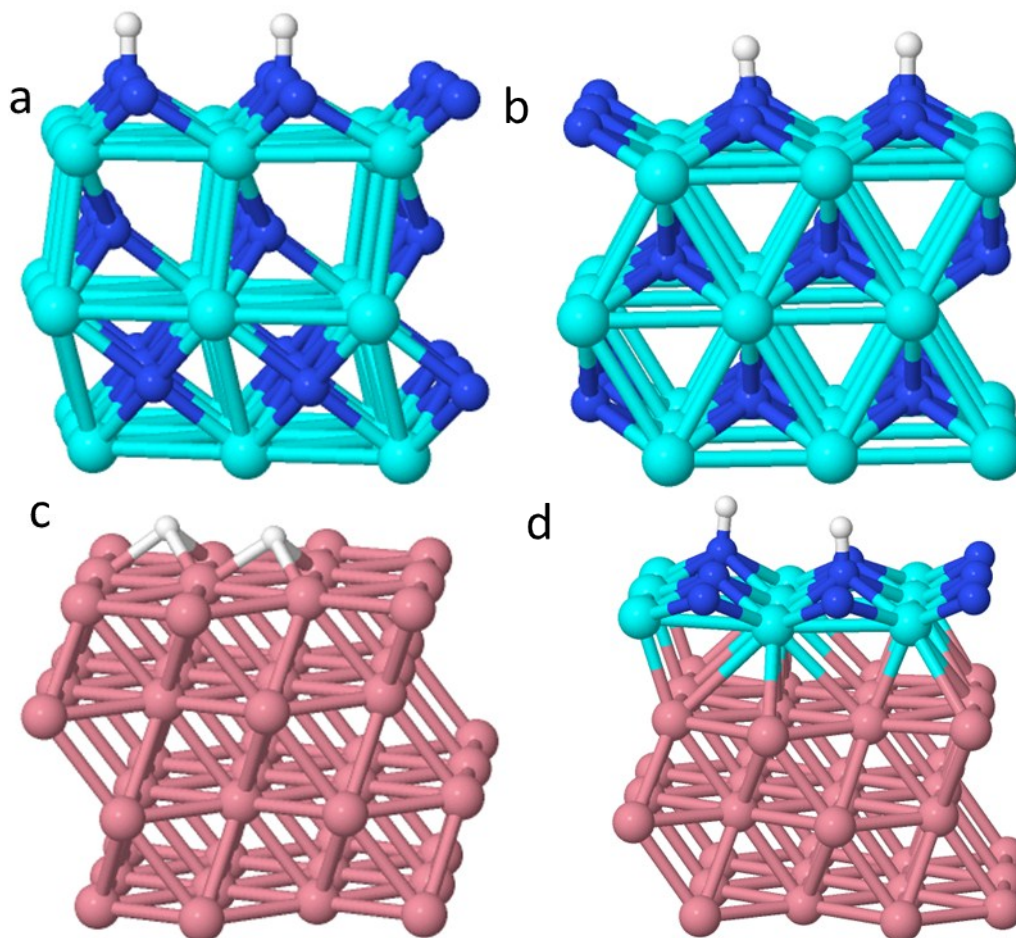


**Figure S4.** H binding ( $1/2ML_H$ ) on (a)  $\beta$ -WN, (b)  $\delta$ -WN, (c) Co and (d)  $\delta$ -WN/Co (blue: nitrogen; cyan: tungsten; white: hydrogen).

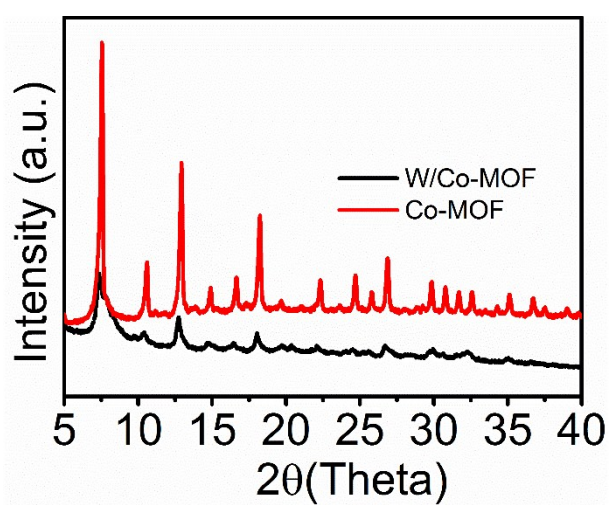


**Figure S5.** X-ray diffraction patterns of ZIF-67 and AMT-doped ZIF-67.

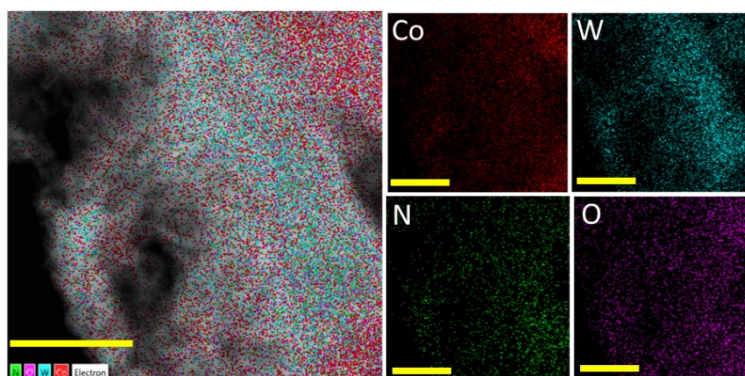


**Figure S6.** STEM-EDS elemental mappings of  $\delta$ -WN/Co, Co (red), W (blue), N (green), O (purple). (Scale bar: 50 nm).

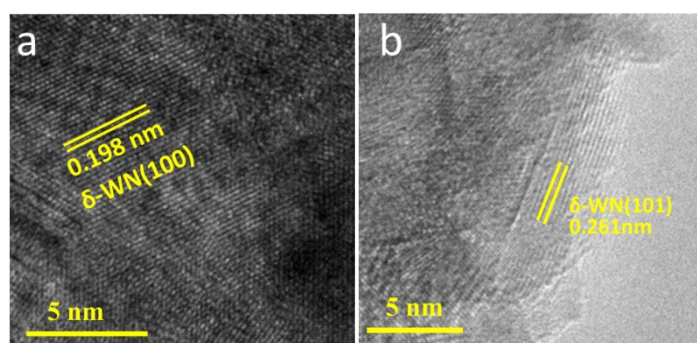


**Figure S7.** The HRTEM images of  $\delta$ -WN in  $\delta$ -WN/Co<sub>2.45</sub>.

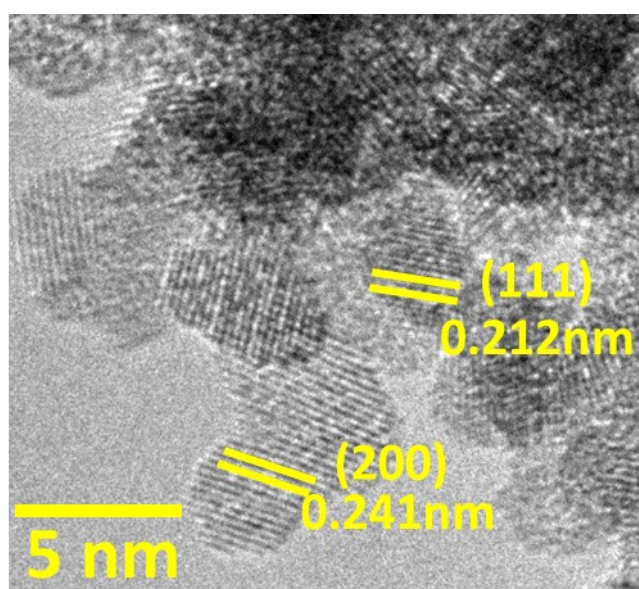


**Figure S8.** HRTEM image of  $\beta$ -WN.

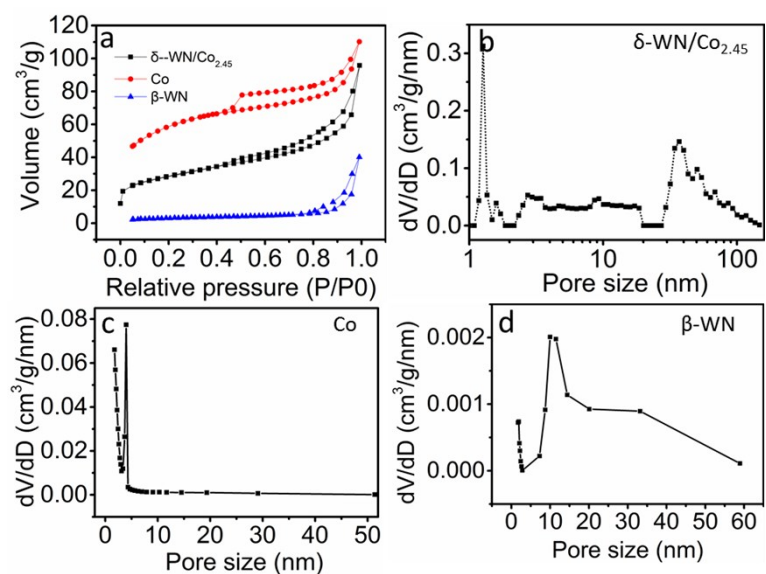


**Figure S9.** (a) N<sub>2</sub> adsorption/desorption isotherms and (b-d) corresponding Barrett-Joyner-Halenda (BJH) pore-size distribution curve determined from the desorption branch of the isotherm of  $\delta$ -WN/Co<sub>2.45</sub>, Co and  $\beta$ -WN.

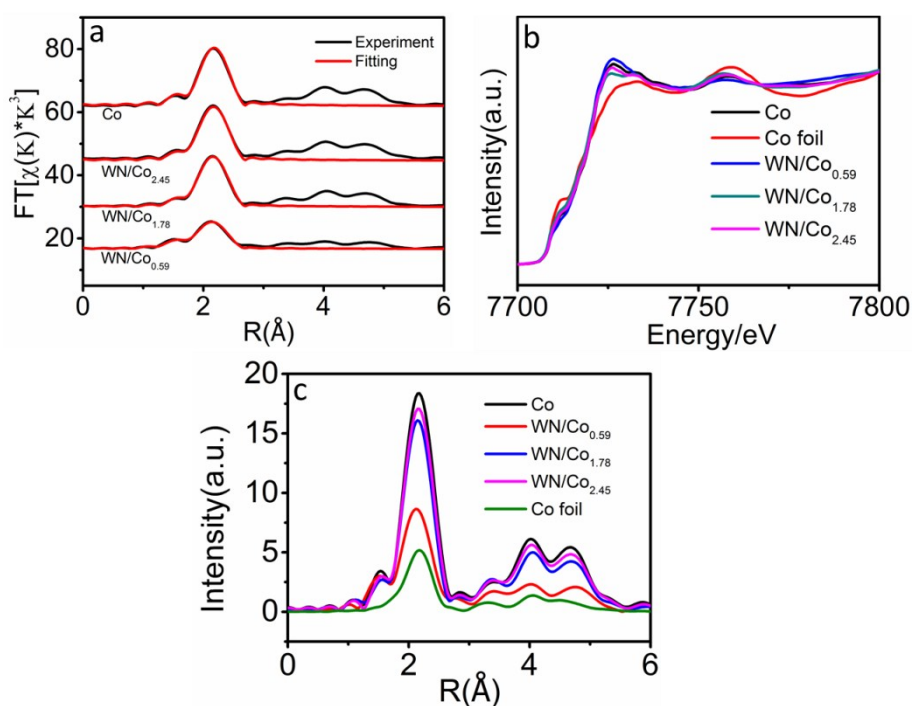


**Figure S10.** a) the Co K-edge EXAFS fitting results, b) XANES spectra, c) EXAFS of catalysts.

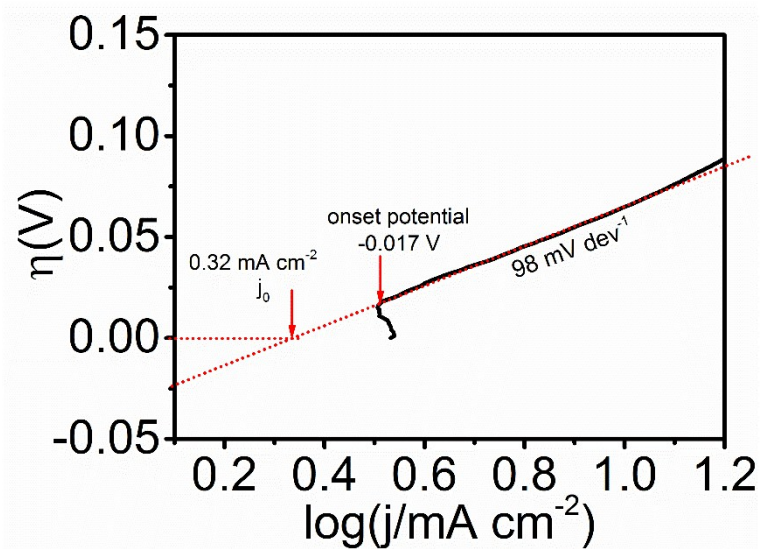


Figure S11. The tafel plots of  $\delta$ -WN/Co<sub>2.45</sub>.

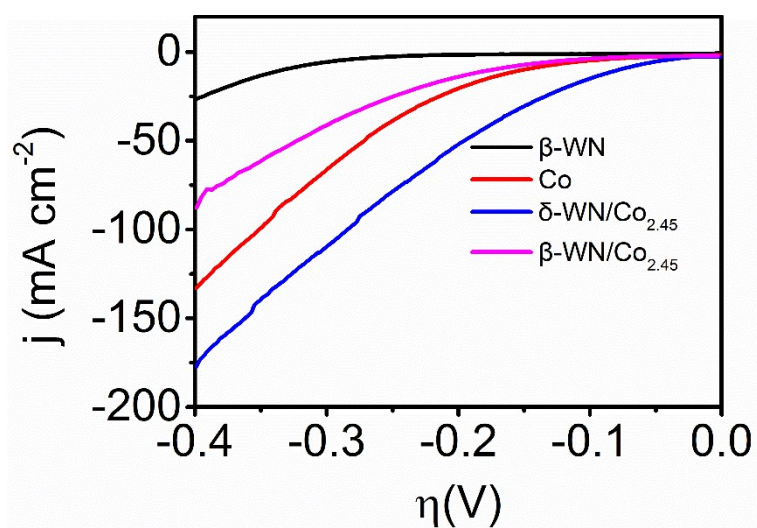
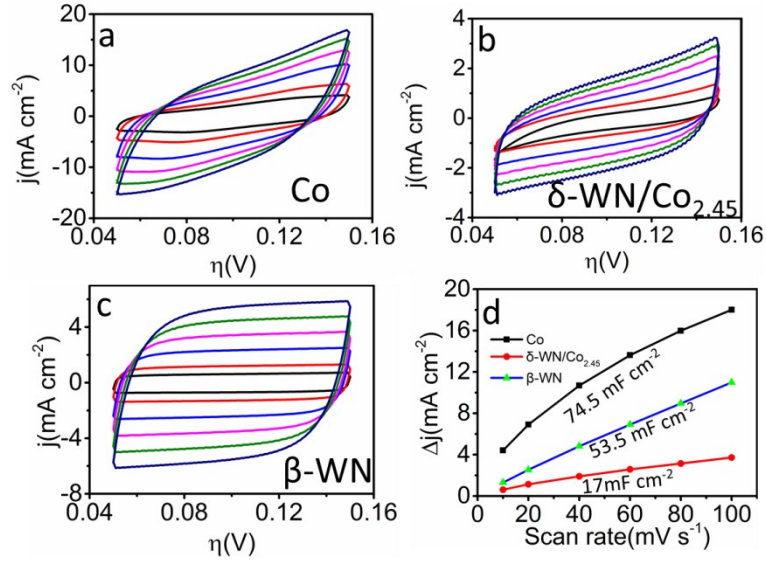
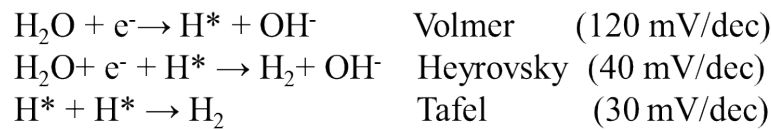


Figure S12. Polarization curves of different catalysts.



**Figure S13.** Typical cyclic voltammetry curves of (a) metallic cobalt, (b)  $\delta$ -WN/ $\text{Co}_{2.45}$  and (c)  $\beta$ -WN; (d)  $\Delta J$  ( $J_a - J_c$ ) of three catalysts plotted against scan rates in 1 M KOH with different scan rates.

The estimation of the effective active surface area of catalysts was realized according to literature. Cyclic voltammetry (CV) were carried out at various scan rates (10, 20, 40 mV s<sup>-1</sup>, etc.) in 0.05-0.15V vs RHE region. The double-layer capacitance ( $C_{dl}$ ) of three samples can be determined from the cyclic voltammograms, which is expected to be linearly proportional to the effective surface area (Figure 12d). The exact determination of the surface area is difficult due to the unknown capacitive behavior of catalysts, but we can safely estimate the relative surface areas. CV measurements performed in the region of 0.05-0.15 V vs RHE could be mostly considered as the double-layer capacitive behavior. The double-layer capacitance is estimated by plotting the  $\Delta J = J_a - J_c$  at 0.1 V vs RHE against the scan rate, where the slope is twice  $C_{dl}$  (Figure 4b). The calculated values of double-layer capacitance are 74.5, 17 and 53.5 mF cm<sup>-2</sup> for Co,  $\delta$ -WN/ $\text{Co}_{2.45}$  and  $\beta$ -WN, respectively.



**Figure S14.** The mechanism of  $\text{H}_2$  evolution in alkaline media.

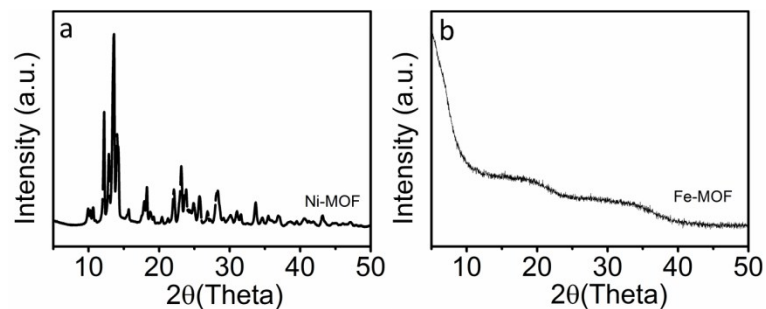


**Figure S15.** X-ray diffraction patterns of Ni-MOF and Fe-MOF.

As observed in Figure S15, the structure of Ni-MOF formed, which is different from the corresponding oxides or hydroxides. The degree of crystallinity for Fe-MOF is too low to produce XRD peaks.

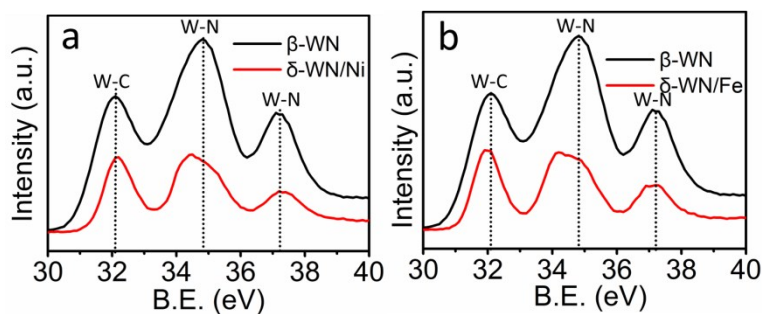


**Figure S16.** XPS spectra of W 4f in  $\delta$ -WN/Ni and  $\delta$ -WN/Fe.

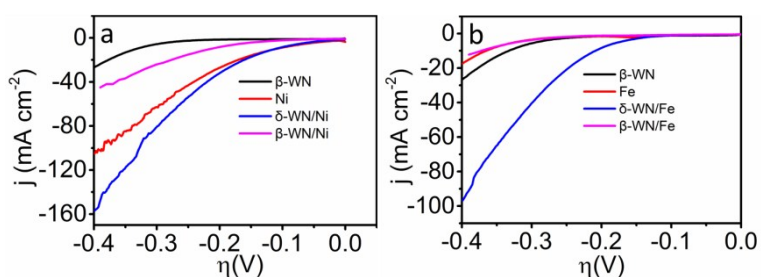


**Figure S17.** Polarization curves of different catalysts.

**Table S1.** The ratio of Co/W in as-prepared catalyst determined by XRF measurement.

Original ratio	1:2	1:1	3:1	5:1	7:1
As-prepared ratio	1:2.55	1:1.68	1.78:1	2.45:1	3.35:1

**Table S2.** the calculated TOF value of  $\delta$ -WN/Co<sub>2.45</sub>, metal Co,  $\delta$ -WN and  $\beta$ -WN.

materials	Metal Co	$\delta$ -WN/Co <sub>2.45</sub>	$\delta$ -WN	$\beta$ -WN
TOF	$2.85 \cdot 10^{-3}$	$19.3 \cdot 10^{-3}$	$16.45 \cdot 10^{-3}$	$0.72 \cdot 10^{-3}$

**Table S3.** The  $\Delta G_H$  on Co and different planes of WN calculated by DFT.

	planes	$\Delta E_H$ (1/4ML <sub>H</sub> )	$\Delta G_H$ (1/4ML <sub>H</sub> )
$\delta$ -WN	(001) N-H	-1.875	-1.635
	W-H	-0.962	-0.722
	<b>(100) N-H</b>	<b>-0.498</b>	<b>-0.258</b>
	W-H <sub>1</sub>	-1.576	-1.336
	W-H <sub>2</sub>	-1.293	-1.053
	(101) N-H	0.692	0.932
W-H	-0.927	-0.687	
(110)	N-H	-0.580	-0.340
	W-H	-1.157	-0.917
<b>Co</b>	<b>(111)</b>	<b>-0.7</b>	<b>-0.46</b>
$\delta$ -WN/Co	<b>(100)</b>	<b>-0.385</b>	<b>-0.145</b>
$\beta$ -WN	<b>(100) N-H</b>	<b>-1.05</b>	<b>-0.81</b>
	W-H	-0.94	-0.7
	(110) N-H	-0.791	-0.551(structural damage)
	W-H	-1.196	-0.956

**Table S4.** The comparison of  $\Delta G_H$  based on different hydrogen adsorption coverage.

	1/4 ML <sub>H</sub>	1/2 ML <sub>H</sub>
$\delta$ -WN (100)	-0.258	-0.185
$\beta$ -WN (100)	-0.81	-0.94
<b>Co (111)</b>	-0.46	-0.445
$\delta$ -WN/Co	-0.145	-0.085

**Table S5.** The  $\Delta E_H$ ,  $\Delta E_{OH}$ ,  $\Delta E_{d-H_2O}$  on Co and WN calculated by DFT.

	$\Delta E_H$ (1/4 ML <sub>H</sub> , on N site)	$\Delta E_{OH}$ (on W sites)	$\Delta E_{d-H_2O}$ (on W sites)
$\delta$ -WN (100)	-0.498	-1.59	-1.57
$\beta$ -WN (100)	-1.05	-0.62	-1.19
<b>Co (111)</b>	-0.7	-0.61	-0.54

**Table S6.** The content of nitrogen in  $\delta$ -WN/Co<sub>2.45</sub> and  $\beta$ -WN.

Name	N [%]	C [%]	H [%]
$\delta$ -WN/Co <sub>2.45</sub>	5.73	0.8	0.29
$\beta$ -WN	6.96	0.08	0.7

**Table S7.** The BET data of catalysts.

samples	D <sub>p</sub> (nm)	V <sub>p</sub> (cm <sup>3</sup> g <sup>-1</sup> )	S <sub>BET</sub> (m <sup>2</sup> g <sup>-1</sup> )
δ-WN/Co <sub>2.45</sub>	6.1	0.15	97
Co	3.5	0.17	196
β-WN	22.1	0.06	11

**Table S8.** The fitting results of W L<sub>3</sub>-edge in δ-WN/Co<sub>2.45</sub>.

Sample	Shell	N	R(Å)	σ <sup>2</sup> (10 <sup>-3</sup> Å <sup>2</sup> )	ΔE <sub>0</sub> (eV)	R-factor
δ-WN	W-N	6.0	2.18			
	W-W	2.0	2.82			
	W-W	6.0	2.89			
β-WN	W-N	4.0	2.06			
	W-W	12.0	2.92			
δ-WN/Co <sub>2.45</sub>	W-N	4.0	2.16	5.2±1.4	12.1±1.8	0.019
	W-W	8.0	2.88	5.2±0.4	8.2±1.6	

N, coordination number; R, distance between absorber and backscatter; σ<sup>2</sup>, Debye–Waller factor; ΔE<sub>0</sub>, energy shift.

**Table S9.** The fitting results of Co K-edge in δ-WN/Co.

Sample	Shell	N	R(Å)	σ <sup>2</sup> (10 <sup>-3</sup> Å <sup>2</sup> )	ΔE <sub>0</sub> (eV)	R-factor
Co	Co-N	1.2±0.2	1.96±0.02	5.0	6.3±0.1	0.003
	Co-Co	7.6±0.6	2.50±0.01	7.1±0.1	6.3±0.1	
δ-WN/Co <sub>0.59</sub>	Co-N	1.2±0.4	1.94±0.02	5.0	1.8±1.0	0.006
	Co-Co	5.2±0.6	2.49±0.01	10.0±1	1.8±1.0	
δ-WN/Co <sub>1.78</sub>	Co-N	0.6±0.2	1.93±0.03	5.0	4.1±0.6	0.002
	Co-Co	8.4±0.5	2.50±0.01	9.0±0.1	4.1±0.6	
δ-WN/Co <sub>2.45</sub>	Co-N	1.1±0.6	1.98±0.03	10.2±10.0	5.5±0.6	0.001
	Co-Co	8.0±0.5	2.50±0.01	8.1±0.1	5.5±0.6	

N, coordination number; R, distance between absorber and backscatter; σ<sup>2</sup>, Debye–Waller factor; ΔE<sub>0</sub>, energy shift.

**Table S10.** Comparison of the electrocatalytic activity of δ-WN/Co<sub>2.45</sub> vis-à-vis metal nitrides and recently reported noble metal-free catalysts.

Catalyst	Catalyst amount (mg)	Current density j	Overpotential (vs. RHE) at the	Reference
----------	----------------------	-------------------	--------------------------------	-----------

	cm <sup>-2</sup> )		corresponding j	
Co-NRCNTs	0.28	10 mA cm <sup>-2</sup>	370 mV	<i>Angew. Chem., Int. Ed.</i> <b>2014</b> , <i>53</i> , 4372. <sup>1</sup>
Co <sub>0.6</sub> Mo <sub>1.4</sub> N <sub>2</sub>	0.24	10 mA cm <sup>-2</sup>	~ 200 mV in 0.1 M HClO <sub>4</sub>	<i>J. Am. Chem. Soc.</i> <b>2013</b> , <i>135</i> , 19186.
NiMoN <sub>x</sub>	0.25	5 mA cm <sup>-2</sup>	~ 225 mV in 0.1 M HClO <sub>4</sub>	<i>Angew. Chem., Int. Ed.</i> <b>2012</b> , <i>51</i> , 6131.
NiMoN/CC	1.1	10 mA cm <sup>-2</sup>	109 mV	<i>Adv. Energy Mater.</i> , <b>2016</b> , <i>6</i> , 1600221.
<b>δ-WN/Co<sub>2.45</sub></b>	<b>1.1</b>	<b>10 mA cm<sup>-2</sup></b>	<b>76</b>	<b><i>This work</i></b>
Fe-WCN	0.4	10 mA cm <sup>-2</sup>	220 mV	<i>Angew. Chem. Int. Ed.</i> <b>2013</b> , <i>52</i> , 13638.
P-WN/rGO	N	10 mA cm <sup>-2</sup>	85 mV	<i>Angew. Chem. Int. Ed.</i> <b>2015</b> , <i>54</i> , 6325. <sup>2</sup>
Co-C-N	N	10 mA cm <sup>-2</sup>	138 mV in 0.5 M H <sub>2</sub> SO <sub>4</sub>	<i>J. Am. Chem. Soc.</i> <b>2015</b> , <i>137</i> , 15070.
CoP <sub>4</sub> N <sub>2</sub>	N	5 mA cm <sup>-2</sup>	~ 750 mV	<i>Angew. Chem., Int. Ed.</i> <b>2011</b> , <i>50</i> , 7238.
NiCN-NSs	0.2	10 mA cm <sup>-2</sup>	31 mV	<i>J. Am. Chem. Soc.</i> <b>2016</b> , <i>138</i> , 14546.
Ni/MWCNT	N	10 mA cm <sup>-2</sup>	~ 350 mV	<i>J. Power Sources</i> <b>2014</b> , <i>266</i> , 365.
CoO <sub>x</sub> @CN	2.1	20 mA cm <sup>-2</sup>	134 mV	<i>J. Am. Chem. Soc.</i> <b>2015</b> , <i>137</i> , 2688.
MoP	0.86	10 mA cm <sup>-2</sup>	~ 150 mV	<i>Energy Environ. Sci.</i> <b>2014</b> , <i>7</i> , 2624.
Co <sub>x</sub> W <sub>1-x</sub> S <sub>2</sub>	~1.7	10 mA cm <sup>-2</sup>	121 mV	<i>small</i> <b>2016</b> , <i>12</i> , 3802.
Commercial MoC	0.21	10 mA cm <sup>-2</sup>	> 250 mV	<i>Energy Environ. Sci.</i> <b>2014</b> , <i>7</i> , 387

## References

- (1) Zou, X.; Huang, X.; Goswami, A.; Silva, R.; Sathe, B. R.; Mikmekova, E.; Asefa, T. *Angew. Chem., Int. Ed.* **2014**, *53*, 4372.
- (2) Vrubel, H.; Hu, X. *Angew. Chem., Int. Ed.* **2012**, *51*, 12703.